ANTICANCER RESEARCH *37*: 5207-5214 (2017)
doi:10.21873/anticanres.11944

Targeted Delivery of Cordycepin to Liver Cancer Cells Using Transferrin-conjugated Liposomes

YE BI[1*], YULIN ZHOU[1*], MENGQIAO WANG[1], LIANLIAN LI[1], ROBERT J. LEE[1,2,3], JING XIE[1] and LESHENG TENG[1,3]

[1]*Jilin University, College of Life Science, P. R. China;*
[2]*Division of Pharmaceutics, College of Pharmacy, The Ohio State University, Columbus, OH, U.S.A.*
[3]*Department of Chemistry, Zhuhai College of Jilin University, Zhuhai, P.R. China*

Abstract. *Background/Aim: Cordycepin is an endogenous nucleoside with significant anticancer biological activity. The objective of this study was to develop targeted liposomes to improve solubility and biological activity of cordycepin. Materials and Methods: We established transferrin-conjugated liposomes to deliver cordycepin to liver cancer cells and evaluated the uptake and effect. Results: The liposomes were loaded with cordycepin. Their average size was 125.3 nm, with drug encapsulation efficiency of 65.3%. The liposomes had good colloidal stability and released cordycepin slowly. Liposomal cordycepin was shown to increase reactive oxygen species production and cause depolarization of the mitochondrial transmembrane in liver cancer cells. Cellular uptake of liposomal cordycepin was enhanced by conjugation to transferrin, that facilitated receptor-mediated endocytosis. Conclusion: Transferrin-conjugated liposomes are effective as nanocarriers for cordycepin delivery to liver cancer cells.*

Liver cancer is the sixth most common cancer worldwide with the second highest fatality rate, and the incidence of liver cancer has been showing an increasing trend. Current treatment, consisting of surgery, trans-arterial chemoembolisation, kinase inhibitor sorafenib, and chemotherapy, all have limited effectiveness (1).

*These Authors contributed equally to this study.

Correspondence to: Robert J. Lee, College of Pharmacy, The Ohio State University, Columbus, Ohio 43210, U.S.A. Tel: +1 6142924172, e-mail: lee.1339@osu.edu; or Lesheng Teng, College of Life Sciences, Jilin University, 2699 Qianjin Avenue, Changchun, Jilin, P.R. China. Tel: +86 43185168646, Fax: +86 43185168637, e-mail: tenglesheng@jlu.edu.cn

Key Words: Cordycepin, liposomes, protamine, cytotoxicity, cell uptake.

Cordyceps, a traditional Chinese herbal medicine, has been shown to prolong the survival of patients with cancer with minimal side-effects (2). Cordycepin (3-deoxyadenosine) is the main active ingredient of cordyceps. It has selective antiproliferative effects on human oral, breast (3, 4), lung (5), prostate (6), and liver cancer cells (7). Cordycepin is an analog of adenosine. It binds to the adenosine A3 receptor, activates glycogen synthase kinase (GSK)-3β, and inhibits cyclin D1, resulting in cell growth inhibition (8). In addition, cordycepin inhibits hepatic metastasis *via* accelerating secretion of tissue inhibitor of metalloproteinase-1 (9), and blocking ADP-induced platelet aggregation (10). Furthermore, cordycepin may inhibit RNA synthesis by inducing premature termination through incorporation of cordycepin triphosphate (11). Finally, cordycepin can activate reactive oxygen species (ROS)-mediated pathways to induce cancer cell apoptosis (8).

Cordycepin has low solubility in water at room temperature, can be degraded by adenosine deaminase, and is rapidly cleared when injected ($t_{1/2}$=1.6 min) in the rat (12, 13). Cordycepin is negative charged and is rejected by cell membranes, which is a disadvantage for cellular uptake. Improvement in formulation is needed to improve solubility and circulation time of this drug.

Liposomes are composed of phospholipids and are an ideal drug delivery vehicle, which has been extensively studied. Compared to free drugs, liposomal drugs prolong blood circulation time. Transferrin (Tf) receptor is overexpressed in many types of tumor cells, including liver cancer cells. Tf-conjugated liposomes (Tf-liposomes) can be used to selectively target drug delivery to cancer cells. In this study, Tf-liposomes were evaluated as delivery vehicles for cordycepin.

Materials and Methods

General experimental procedures. Hydrogenated soy phosphatidylcholine (HSPC), cholesterol, 1,2-distearoyl-sn-glycero-

3-phosphoethanolamine-*N*-[methoxy (polyethylene glycol)-2000] (DSPE-mPEG2000) were purchased from Lipoid GmbH (Ludwigshafen, Rheinland-Pfalz, Germany). 2',7'-Dichlorodihydrofluorescein diacetate (DCFH-DA), a fluorescent dye, was obtained from Nanjing Jiancheng Bioengineering Institute (Nanjing, P.R. China). 5,5',6,6'-Tetrachloro-1,1',3,3'-tetraethylbenzimidazolylcarbocyanine iodide (JC-1), 7-nitrobenzofurazan-labeled 1,2-dioleoyl-*sn*-glycero-3-phosphoethanolamine (NBD-DOPE), sulforhodamine B, and human holo-transferrin (holo-Tf) were purchased from Sigma-Aldrich (St. Louis, MO, USA). 4',6-Diamidino-2-phenylindole (DAPI) was purchased from Molecular Probes Inc. (Eugene, OR, USA). PLC/PRF/5 and HepG2 cell lines were purchased from the American Type Culture Collection (Manassas, VA, USA).

Preparation and characterization of Tf-liposomes. We used an ethanol dilution-sonication method to prepare Tf-liposomes. Firstly, HSPC/PEG-DSPE/cholesterol (mass ratio=3:1:1) were dissolved in ethanol at 10 mg/ml. It was injected into protamine aqueous solution (2 mg/ml) at 65˚C (volume ratio=1:2) under vortex mixing and liposomes were dialyzed; cordycepin solution was added to the previous step solution under vortex mixing for 30 s, sonicated for 30 s to obtain cordycepin liposomes (LP-cordycepin) (14). The LP-cordycepin was then incubated at 4˚C for 24 h for physical absorption. Secondly, the liposomes were dialyzed to remove unencapsulated agent and ethanol, and concentrated by ultrafiltration (MWCO 10 kDa). Finally, the liposomes were incubated with Tf-PEG-DSPE (mass ratio of transferrin and lipid =1:500) at 37˚C for 1 h to prepare Tf-LP-cordycepin (15).

We used NBD-DOPE (1% mole of total lipids) to label the lipid membrane and sulforhodamine B (10 mM) to label the aqueous phase for preparing double-labeled liposomes (16).

Characterization of liposomes. The size distribution and zeta potential of Tf-LP-cordycepin were determined using a Zetasizer Nano ZS 90 (Malvern Instruments, Ltd., Malvern, UK) by quasielastic light scattering in intensity-weighted Gaussian size distribution mode at 25˚C.

A JEOL JSM-6700F field emission scanning electron microscopy (SEM) (Tokyo, Japan) was used to observe the surface morphology of Tf-LP-cordycepin at 3 kV accelerating voltage. The images were acquired in secondary electron mode (17).

Entrapment efficiency (EE%) is a crucial parameter that determines the pharmacodynamics and pharmacokinetic behavior of liposome-encapsulated drugs. EE% was measured by ultrafiltration-centrifugation methods. Firstly, the liposomes were destroyed by 3% Triton X-100 to measure the total cordycepin (T_{drug}). Secondly, unencapsulated cordycepin (F_{drug}) was separated using ultrafiltration centrifuge tube (MWCO 10-kDa) for 30 min at 4˚C at 12,857 × *g*. Cordycepin concentration was determined at 260 nm through a Agilent SB-C18 column (4.6 mm × 250 mm, 5 μm) with a mobile phase of methanol/water (15:85, v/v%) at a flow rate of 1 ml/min at 35˚C. Finally, a 20 μl sample of the solution was injected into a Waters E2695 HPLC system (Milford, MA, USA) to measure F_{drug} and T_{drug}.

$$EE\% = \frac{T_{drug} - F_{drug} \times 100\%}{T_{drug}}$$

In vitro release. Tf-LP-cordycepin was placed in a dialysis bag (MW cut off 8- to 12-kDa) to evaluate the release rate of cordycepin from liposomes. The dialysis bag containing 2 mg cordycepin was soaked in 200 ml phosphate-buffered saline (PBS) at 37˚C with stirring at 300 rpm, 0.5 ml of the release medium was withdrawn at pre-determined time points, and replaced by an equal volume of fresh PBS solution. The concentration of cordycepin released into the release medium was determined by the aforementioned HPLC method. The percentage of cumulative cordycepin release from liposomes were calculated (n=3) (5).

Table I. *Particle size and zeta potential of cordycepin suspension, LP-cordycepin and Tf-LP-cordycepin.*

	Cordycepin	LP-cordycepin	Tf-LP-cordycepin
Particle size	Not determined	91.2±3.1 nm	125.3±2.2 nm
Zeta potential	−23.2±3.1 mV	+9.2±3.5 mV	+2.9±2.4 mV

Cytotoxicity assay. The cytotoxicity of cordycepin and its preparations were measured using the 3-(4,5-dimethylthiazol-2-yl)-2,5-diphenyl tetrazolium bromide (MTT) assay. The PLC/PRF/5 or HepG2 cells were plated in 96-well plates at 10^4 cells per well with 100 μl Dulbecco's modified Eagle's medium containing 10% fetal bovine serum and cultured for 24 h. The cells were then incubated with cordycepin, liposomes or Tf-LP-cordycepin for another 24 h at 37˚C in a humidified atmosphere containing 5% CO_2, then 10 μl of MTT (5 mg/ml) was added to each well and cells further incubated for 4 h. The medium was replaced by 150 μl dimethylsulfoxide to dissolve formazan crystals and the absorbance was measured at 490 nm by a microplate reader. The results of these tests were analyzed to yield half maximal inhibitory concentration (IC_{50}) values.

Assessment of production of ROS. The PLC/PRF/5 or HepG2 cells were plated in 6-well plates at a density of 2×10^5 cells per well. After exposure to 30 μM cordycepin, LP-cordycepin or Tf-LP-cordycepin for 12 h, the cells were incubated with 10 μM DCFH-DA to stain at 37˚C for 10 min in darkness (8, 18). Images were then obtained by inverted fluorescent microscopy.

Mitochondrial transmembrane potential ($\Delta\Psi m$) assay. The PLC/PRF/5 or HepG2 cells were seeded in 6-well plates at a density of 2×10^5 cells per well to culture for 24 h. They were then incubated with 30 μM of cordycepin, LP-cordycepin or Tf-LP-cordycepin for 12 h. Cells were subsequently washed with PBS, and then 10 μg/ml of JC-1 dissolved in culture medium was added to the culture and cells were further incubated for 37˚C in the dark for 30 min. After the medium was replaced by fresh medium, mitochondrial membrane depolarization was measured through the red fluorescent/green fluorescent intensity ratio using an inverted fluorescent microscope. The intensity of fluorescent was determined by imaging software Image J (19).

Confocal microscopy and analysis of cellular internalization. PLC/PRF/5 and HepG2 cells (1×10^5 cells per well) were plated in a 35 mm diameter glass-bottom culture dish for 24 h at 37˚C in 5% CO_2. The medium was then removed and fresh medium containing

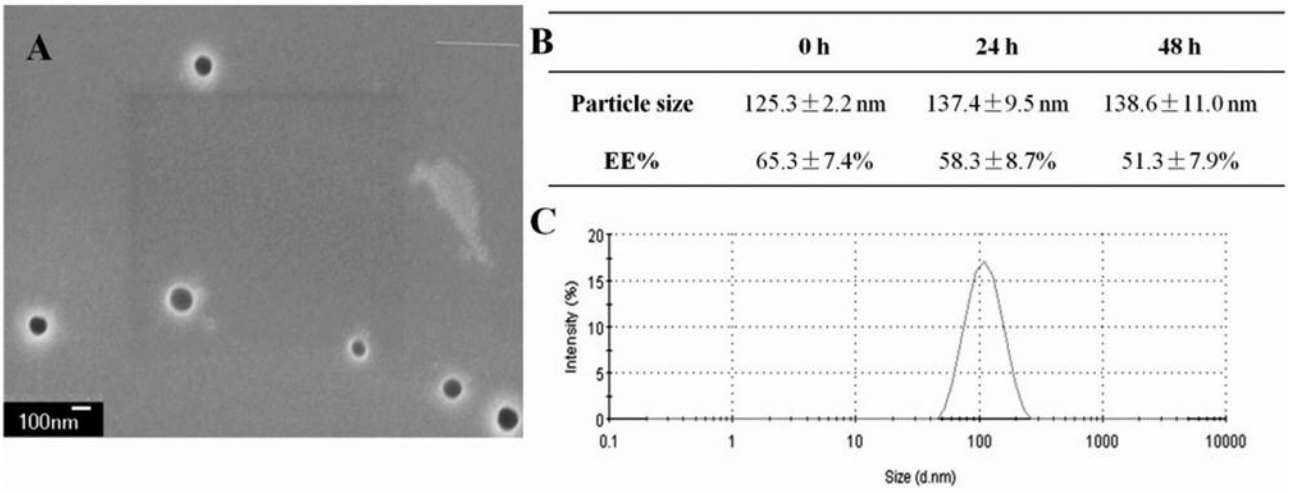

Figure 1. *Characterization of cordycepin-carrying transferrin-conjugated liposomes (Tf-LP-cordycepin). A: Scanning electron micrographs of Tf-LP-cordycepin (×10,000) at 3 kV accelerating voltage. B: Stability of Tf-LP-cordycepin at 25˚C (n=3). C: Distribution of particle size. The mean particle size was ~125 nm, polydispersity index was 0.106.*

LP-cordycepin or Tf-LP-cordycepin was added and cells incubated for 4 h. The cells were then washed with PBS and fixed by 350 μl of 4% paraformaldehyde for 10 min, then cells were washed again. DAPI dye (2 μg/ml) was used to stain the nuclei for 10 min. Dye solution was replaced by PBS, and the cells were immediately observed using a Zeiss 710 LSMNLO confocal microscope (Carl Zeiss, Jena, Germany).

Uptake of LP-cordycepin and Tf-LP-cordycepin. PLC/PRF/5 and HepG2 cells (2×10^5 cells per well) were plated in 6-well plates to culture 24 h with 10% fetal bovine serum-containing medium, and then cells were incubated with 30 μM LP-cordycepin, Tf-LP-cordycepin or Tf-LP-cordycepin (containing human holo-Tf) with culture medium for another 4 h. All the liposome preparations were labeled by NBD-DOPE and sulforhodamine B. The cells were washed with ice-cold PBS (pH 7.4) three times and harvested using 150 μl trypsin, and fixed in 350 μl of 4% formaldehyde solution. The fluorescence intensity was measured by an EPICS XL flow cytometer (Beckman Coulter Corp., Brea, CA, USA) after cell uptake of double-labeled liposomes.

Treatment with inhibitors. PLC/PRF/5 and HepG2 cells were seeded at 2×10^5 cells per well in 6-well plates to culture for 24 h. Cells were then exposed to 0.4 M of sucrose, 5 μM of cytochalasin D or 50 μM of nystatin for 1 h, which were dissolved in culture medium. Fluorescent labeled LP-cordycepin and Tf-LP-cordycepin were added and the cells were incubated for a further 4 h. Finally, the cells were washed with PBS for three times and harvested using 150 μl trypsin, and fixed with 350 μl of 4% formaldehyde solution. The mean fluorescence intensity was used to evaluate the inhibition of uptake (20).

Statistical analysis. The statistical significance of data was analyzed by Student's *t*-test. A *p*-value of <0.05 was accepted as indicating a significant difference. The results are shown as the mean±SD.

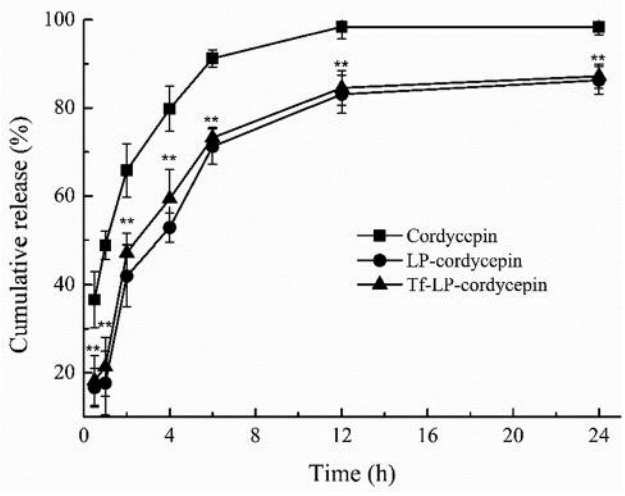

Figure 2. *In vitro release of cordycepin preparations. The cumulative release of cordycepin from free drug suspension, liposomal (LP)-cordycepin and cordycepin-carrying transferrin-conjugated liposomes (Tf-LP-cordycepin) after incubation in phosphate-buffered saline (pH 7.4) was determined at 37˚C. **Release differed significantly at p<0.01 (Tf-LP-cordycepin versus cordycepin suspension).*

Results

Solubility of cordycepin was found to be less than 0.5 mg/ml in water and in ethanol at 25˚C. In addition, using an HPLC method, cordycepin was shown to be stable for >10 min and to have increased solubility (>3 mg/ml) at 65˚C.

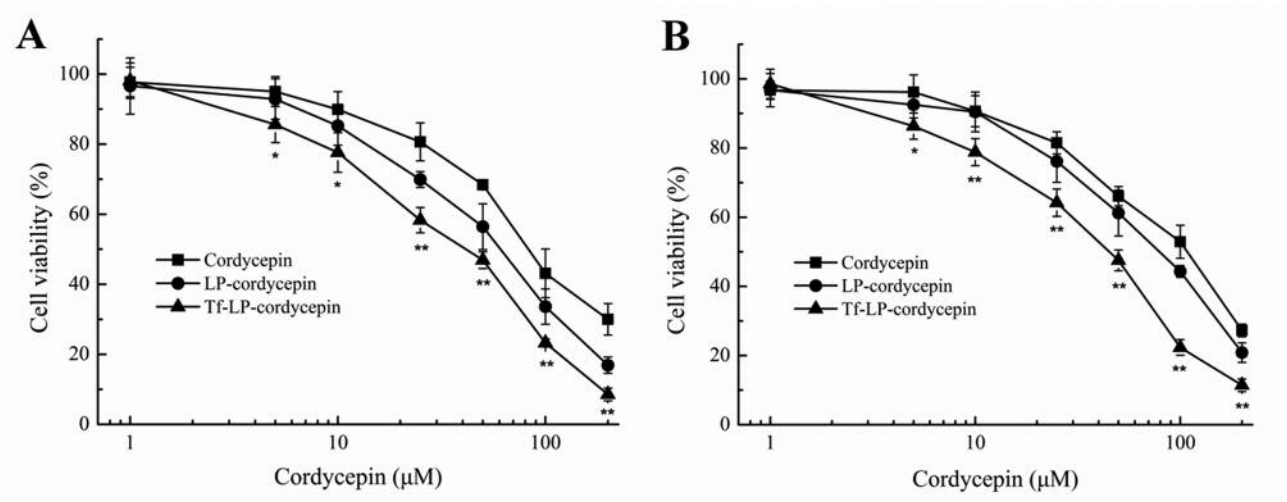

Figure 3. *Cytotoxicity of cordycepin preparations. Cytotoxicity of cordycepin, liposomal (LP)-cordycepin and cordycepin-carrying transferrin-conjugated liposomes (Tf-LP-cordycepin) were determined in Hep G2 (A) and PLC/PRF/5 cells (B) (n=6) by MTT assay. Cellular viability was shown to be significantly different among treatment groups as indicated, at *p<0.05 and **p<0.01 (Tf-LP-cordycepin versus LP-cordycepin).*

Particle size and zeta potential of LP-cordycepin and Tf-LP-cordycepin are shown in Table I. SEM images and colloidal stability of Tf-LP-cordycepin at 25˚C are shown in Figure 1. Liposomes had relatively uniform sizes, smooth surface, and morphology close to spherical.

HPLC methods were developed to determine the concentration of cordycepin. The least-squares linear regression constants (R^2) for cordycepin calibration curves obtained was more than 0.99 in the concentration range of 0.1-200 μg/ml. The retention time of cordycepin was 9 min and protamine did not affect detection of cordycepin. The EE% of cordycepin was 65.3±7.4%.

The *in vitro* release characteristics of cordycepin, LP-cordycepin and Tf-LP-cordycepin are shown in Figure 2. Cordycepin was released faster from free cordycepin suspension than from liposomal preparations. Free cordycepin suspension released about 85% within 4 h, but LP-cordycepin and Tf-LP-cordycepin had released only about 80% of the drug after 24 h.

Tumor cell lines HepG2 and PLC/PRF/5 were used to evaluate the cytotoxicity of cordycepin preparations using an MTT assay. The results are shown in Figure 3. All cordycepin formulations significantly inhibited liver cancer cell growth. The IC_{50} values for cordycepin, LP-cordycepin, and Tf-LP-cordycepin in HepG2 cells were 96, 53 and 31 μM, respectively, at 24 h. Similar data were obtained in PLC/PRF/5 cells, with IC_{50} values of 108, 74 and 35 μM, respectively.

The ROS levels in cancer cells treated with 30 μM cordycepin, LP-cordycepin or Tf-LP-cordycepin are shown in Figure 4. The cellular ROS level increased in the order of cordycepin<LP-cordycepin<Tf-LP-cordycepin, based on observed fluorescence intensity indicating ROS production.

The results of mitochondrial membrane potential changes in the two tumor cell lines (PLC/PRF/5 and HepG2) treated with cordycepin, LP-cordycepin, Tf-LP-cordycepin are shown in Figures 5 and 6. The green fluorescence seen in Figure 5 indicates mitochondrial depolarization. We quantitatively analyzed the degree of mitochondrial depolarization through red/green fluorescence intensity ratio after treatment (Figure 6). Tf-LP-cordycepin had the lowest fluorescence ratio (PLC=0.51, HepG2=0.26), showing it significantly enhanced the degree of mitochondrial membrane potential depolarization compared with the other treatments, which may be one reason for the high cytotoxicity of the Tf-LP-cordycepin preparation.

Confocal microscopy was used to visually analyze the uptake of LP-cordycepin and Tf-LP-cordycepin (Figure 7). PLC/PRF/5 and HepG2 cells were treated with double-labeled LP-cordycepin or Tf-LP-cordycepin to obtain fluorescent images.

The fluorescent images indicate that the lipid and aqueous phases of liposomes were internalized into cells. Tf-LP-cordycepin had higher intracellular localization than LP-cordycepin after 4-h exposure, which was likely due to Tf receptor-mediated uptake. Non-targeted liposomes delivered relatively less drug to cells. In addition, the cells exposed to Tf-LP-cordycepin had reduced growth compared with those treated with LP-cordycepin, which was consistent with the cytotoxicity assay. The results suggest that Tf-LP-cordycepin is an efficient delivery vehicle for cordycepin.

Cellular uptake experiments were used to further investigate whether the improved cytotoxicity of cordycepin

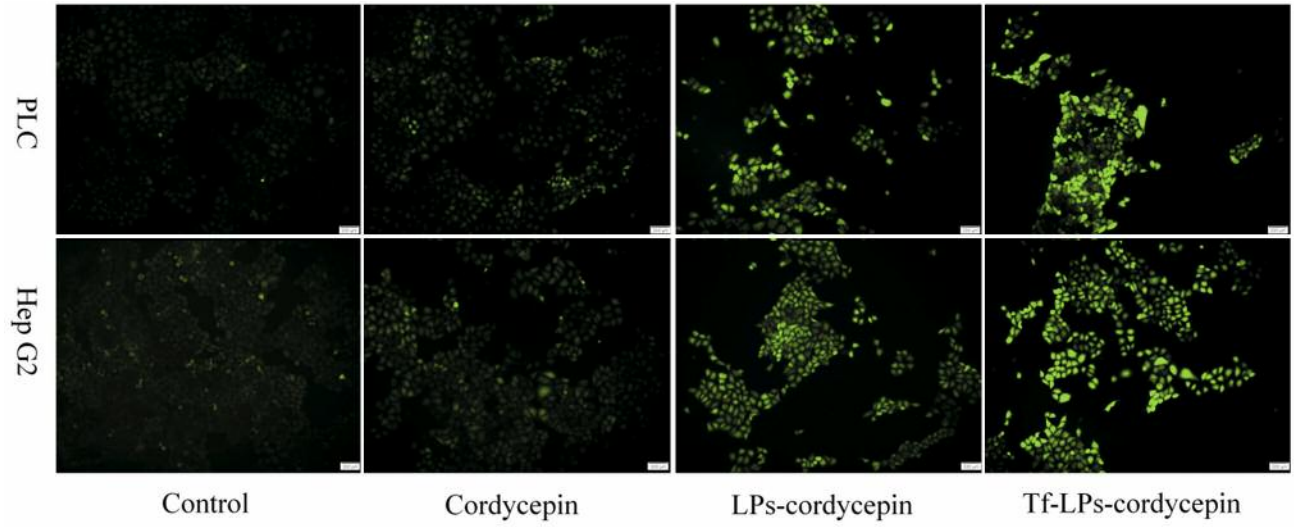

Figure 4. *Production of reactive oxygen species (ROS) by cancer cells after treatment with cordycepin preparations. Hep G2 and PLC/PRF/5 cells were incubated with cordycepin, liposomal (LP)-cordycepin and cordycepin-carrying transferrin-conjugated liposomes (Tf-LP-cordycepin) and the generation of ROS was determined. ROS induction in cells by Tf-LP-cordycepin treatment was significantly greater (greater green fluorescence).*

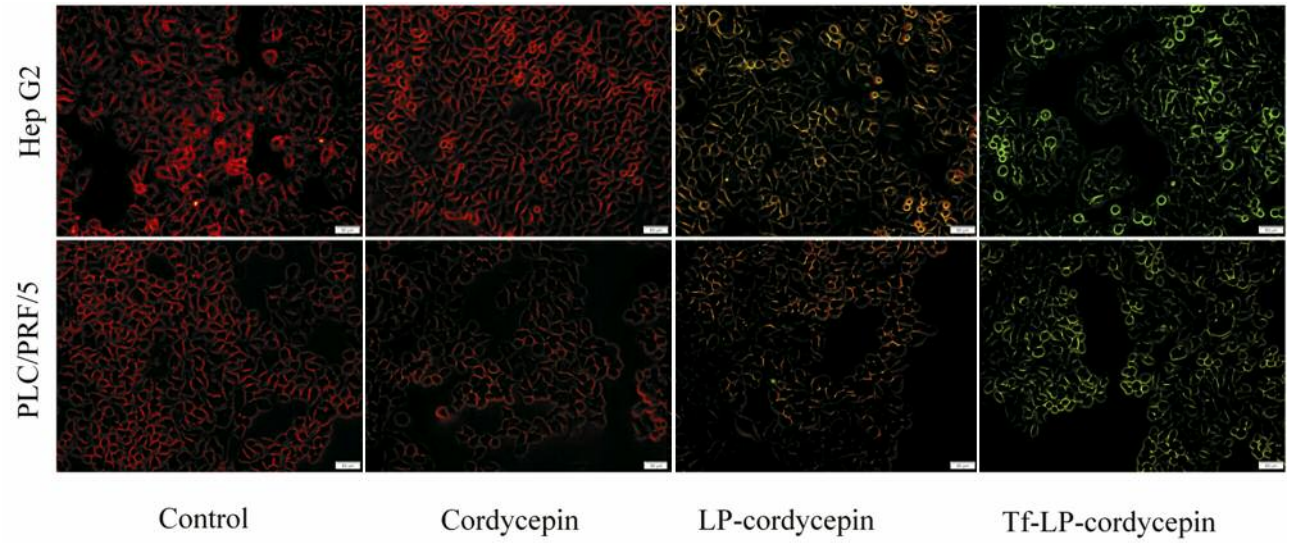

Figure 5. *Mitochondrial transmembrane potential changing after treatment with cordycepin preparations. Merged images of red/green fluorescence after treating two cancer cell lines with cordycepin, liposomal (LP)-cordycepin and cordycepin-carrying transferrin-conjugated liposomes (Tf-LP-cordycepin) are shown. The green fluorescence gradually increased according to the order: control < cordycepin < LP-cordycepin < Tf-LP-cordycepin.*

was associated with Tf-mediated cellular internalization. The cellular uptake of LP-cordycepin and Tf-LP-cordycepin is shown in Figure 8. The mean fluorescent intensity was 2.6 after incubating cells with LP-cordycepin. The mean fluorescent intensity increased to about 12 for cells treated with Tf-modified liposomes. In order to determine whether the increase in uptake was mediated by Tf receptor (TfR), 10 μM holo-Tf was added to cells to saturate TfR before treatment with Tf-LP-cordycepin. The mean fluorescent intensity was reduced by more than 50% with addition of holo-Tf. These data demonstrate that Tf-LP-cordycepin increased uptake efficacy by TfR-mediated targeting *in vitro*.

To investigate the specific mechanism of cellular internalization, endocytosis inhibitors were used to block

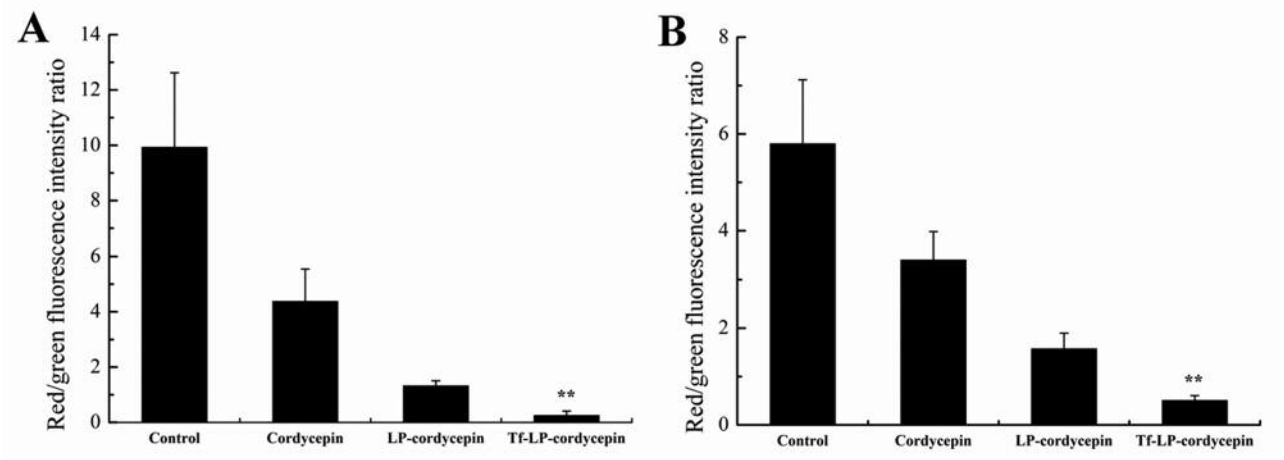

Figure 6. *Red/green fluorescence intensity ratio of cells after treatment with cordycepin preparations. The red/green fluorescence intensity ratio in HepG2 (A) and PLC/PRF/5 (B) cells after treatment with cordycepin, liposomal (LP)-cordycepin and cordycepin-carrying transferrin-conjugated liposomes (Tf-LP-cordycepin) were quantitatively analyzed. All treatments induced mitochondrial transmembrane potential changing, although Tf-LP-cordycepin had the most significant effect. **Significantly different at p<0.01 (Tf-LP-cordycepin versus LP-cordycepin).*

clathrin-mediated endocytosis (with sucrose), marcropinocytosis (with cytochalasin D), and caveolae-mediated endocytosis (with nystatin) (Figure 9). In two cancer cell lines, the uptake of Tf-LP-cordycepin was reduced when pathways of endocytosis were blocked. Sucrose had the most effect on uptake, with about 70% inhibition.

Discussion

In our previous studies, we that found cordycepin has significant therapeutic effect for liver cancer through altering mitochondrial function and increasing ROS, which induce apoptosis (21). Pharmacokinetic results suggest that cordycepin in plasma rapidly decreased at 30 min after administration (13). Since cordycepin is rapidly metabolized and lacks tumor selective uptake, it is difficult to achieve effective concentrations for treatment.

TfR expression is up-regulated in metastatic and drug-resistant tumor cells. In this study, we used TfR-targeting liposomes to improve cordycepin delivery. To facilitate drug loading, cordycepin, which is negatively charged, was electrostatically complexed to protamine (a cationic peptide), and then loaded into liposomes. The final composition carried a net positive charge. Tf was introduced as a targeting ligand in the form of Tf-PEG-DSPE.

The liposome particle size was found to be about 120 nm, allowing them to passively accumulate in tumor tissue based on the enhanced permeability and retention effect.

The IC_{50} value of Tf-LP-cordycepin in 2 liver cancer cell lines were significantly lower than those for cordycepin and LP-cordycepin, which suggests Tf modification enhanced the cellular uptake of liposomes.

Redox signaling plays an important role in regulating cell apoptosis (22). Intracellular accumulation of ROS can change the mitochondrial transmembrane potential. LP-cordycepin was shown to induce high levels of ROS, and Tf-LP-cordycepin was even more effective. ROS generation is likely responsible for the induction of apoptosis in tumor cells.

The expression level of TfR is elevated in malignant tumor (23), sometimes by as much as 100-fold (24). Here, loading into Tf-modified liposomes substantially increased the cytotoxicity of cordycepin compared with LP-cordycepin. Tf-LP-cordycepin would be internalized by cancer cells *via* Tf-mediated endocytosis pathways. Sucrose had the highest inhibitory effect on cordycepin internalization. This indicates that clathrin-mediated endocytosis is the predominant pathway.

Conclusion

Our previous work suggested that cordycepin is a promising anticancer agent, although the molecular mechanisms of anticancer effects were not completely elucidated. In this study, TfR-targeting liposomes were used to improve the delivery of cordycepin to tumor cells. The liposomes clearly increased the antitumor activity of cordycepin through enhanced cell uptake. In future work, we plan to further evaluate the pharmacodynamics and pharmacokinetics of Tf-LP-cordycepin *in vivo*.

References

1 Arii S, Yamaoka Y, Futagawa S, Inoue K, Kobayashi K, Kojiro M, Makuuchi M, Nakamura Y, Okita K and Yamada R: Results of surgical and nonsurgical treatment for small-sized hepatocellular carcinomas: A retrospective and nationwide survey in Japan. Hepatology *32(6)*: 1224, 2000.

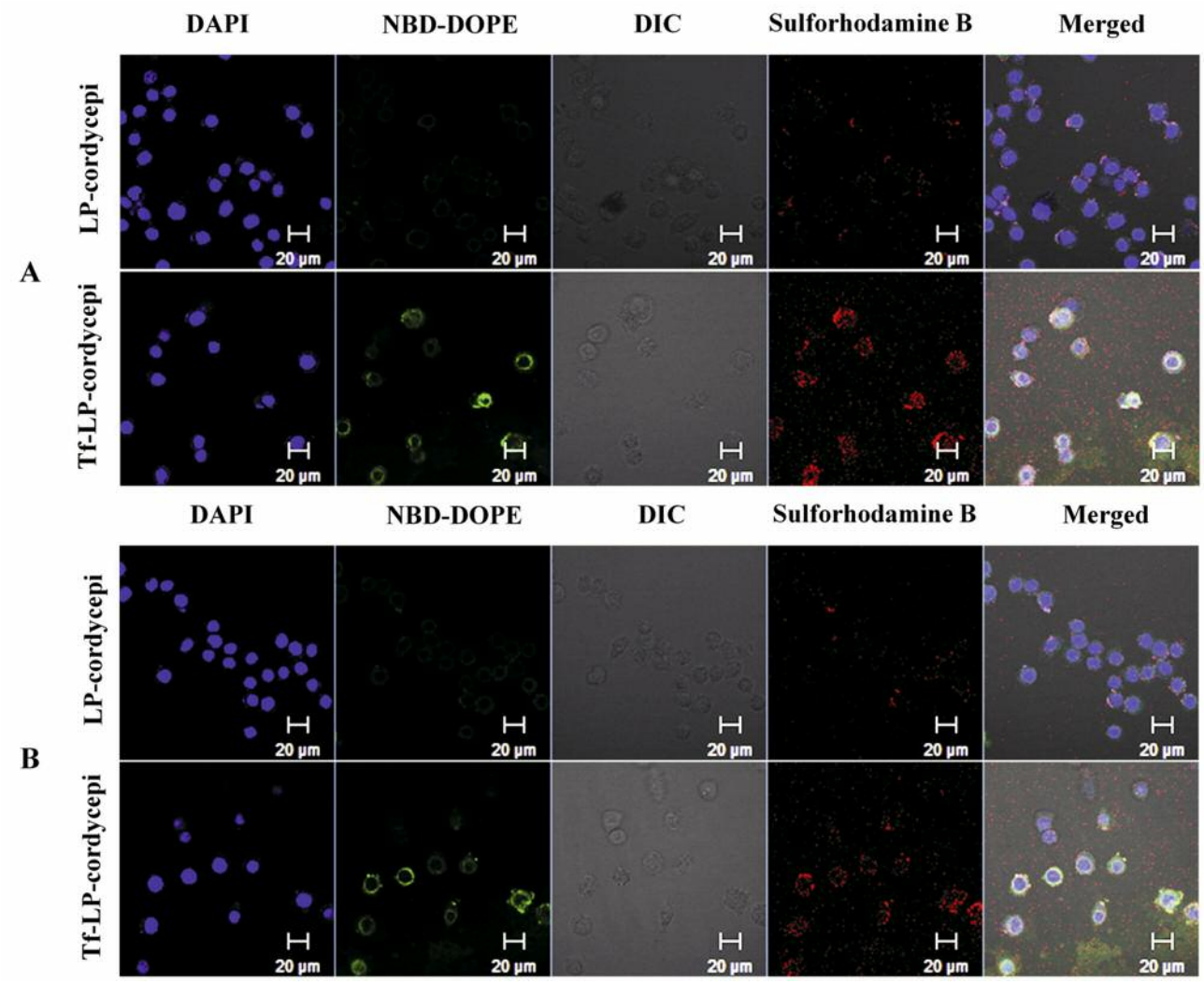

Figure 7. *Cellular uptake of liposomal (LP)-cordycepin and cordycepin-carrying transferrin-conjugated liposomes (Tf-LP-cordycepin). Intracellular localization of LP-cordycepin and Tf-LP-cordycepin is shown. Confocal microscopic images of PLC/PRF/5 cells (A) and HepG2 cells (B) were obtained after 4 h incubation with LP-cordycepin and Tf-LP-cordycepin. Differential interference contrast microscope (DIC) images of matching fields are also shown. DAPI: 4',6-Diamidino-2-phenylindole; NBD-DOPE: 7-nitrobenzofurazan-labeled 1,2-dioleoyl-sn-glycero-3-phosphoethanolamine.*

2 Tuli HS, Sandhu SS and Sharma AK: Pharmacological and therapeutic potential of cordyceps with special reference to cordycepin 3. Biotech *4(1)*: 1, 2014.

3 Foss FM: Combination therapy with purine nucleoside analogs. Oncology *14(6 Suppl 2)*: 31-35, 2000.

4 Thomadaki H, Tsiapalis C and Scorilas A: Polyadenylate polymerase modulations in human epithelioid cervix and breast cancer cell lines, treated with etoposide or cordycepin, follow cell cycle rather than apoptosis induction. J Biol Chem *386(5)*: 471-480, 2005.

5 Aramwit P, Porasuphatana S, Srichana T and Nakpheng T: Toxicity evaluation of cordycepin and its delivery system for sustained *in vitro* anti-lung cancer activity. Nanoscale Res Lett *10(1)*: 1-10, 2015.

6 Lee HH, Kim SO, Kim GY, Moon SK, Kim WJ, Jeong YK, Yoo YH and Choi YH: Involvement of autophagy in cordycepin-induced apoptosis in human prostate carcinoma Ln Cap cells. Environ Toxicol Pharm *38(1)*: 239-250, 2014.

7 Zhou Y, Guo Z, Meng Q, Lu J, Wang N, Liu H, Liang Q, Quan Y, Wang D and Xie J: Cordycepin affects multiple apoptotic pathways to mediate hepatocellular carcinoma cell death. Anti-Cancer Agent Me 16(999), 2016.

8 Lee HH, Park C, Jeong JW, Kim MJ, Seo MJ, Kang BW, Park JU, Kim GY, Choi BT and Choi YH: Apoptosis induction of

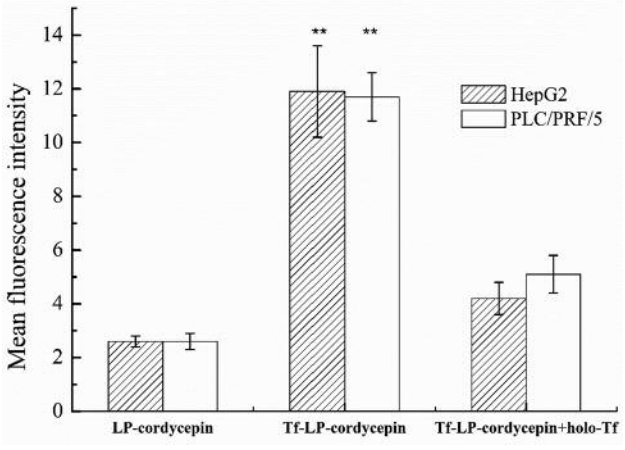

Figure 8. *Cellular fluorescence uptake of liposomal (LP)-cordycepin and cordycepin-carrying transferrin-conjugated liposomes (Tf-LP-cordycepin). The cellular uptake of LP-cordycepin, Tf-LP-cordycepin and Tf-LP-cordycepin with holo-Tf in vitro were measured by flow cytometry. Data represent the mean standard deviation. **Significantly different at p<0.01 (Tf-LP-cordycepin versus Tf-LP-cordycepin+holo-Tf).*

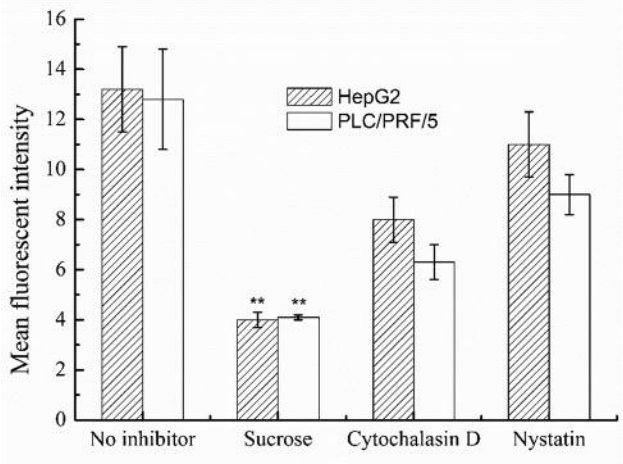

Figure 9. *The influence of endocytosis inhibitors on the internalization of cordycepin-carrying transferrin-conjugated liposomes (Tf-LP-cordycepin). Endocytosis inhibitors (sucrose, cytochalasin D, nystatin) were used to investigate endocytosis mechanism of Tf-LP-cordycepin (n=3). **Significance different at p<0.01 (sucrose versus cytochalasin D).*

human prostate carcinoma cells by cordycepin through reactive oxygen species-mediated mitochondrial death pathway. Int J Oncol *42(3)*: 1036, 2013.

9 Kubo E, Sato A, Yoshikawa N, Kagota S, Shinozuka K and Nakamura K: Effect of *Cordyceps sinensis* on TIMP-1 secretion from mouse melanoma cell. Cent Eur J Biol *7(1)*: 167-171, 2012.

10 Yoshikawa N and Kunitomo MS: Inhibitory effect of cordycepin on hematogenic metastasis of B16-F1 mouse melanoma cells accelerated by adenosine-5'-diphosphate. Anticancer Res *29(10)*: 3857-3860, 2009.

11 Siev M, Weinberg R and Penman S: The selective interruption of nucleolar RNA synthesis in hela cells by cordycepin. J Cell Biol *41(2)*: 510, 1969.

12 Yoshikawa N, Nakamura K, Yamaguchi Y, Kagota S, Shinozuka K and Kunitomo M: Reinforcement of antitumor effect of *Cordyceps sinensis* by 2'-deoxycoformycin, an adenosine deaminase inhibitor. In Vivo *21(2)*: 291, 2007.

13 Tsai YJ, Lin LC and Tsai TH: Pharmacokinetics of adenosine and cordycepin, a bioactive constituent of *Cordyceps sinensis* in Rat. J Agric Food Chem *58(8)*: 4638-4643, 2010.

14 Li Y, Lee RJ, Yu K, Ye B, Qi Y, Sun Y, Li Y, Jing X and Teng L: Delivery of sirna using lipid nanoparticles modified with cell penetrating peptide. Acs Appl Mater Inte *8(40)*: 26613-26621, 2016.

15 Chiu SJ, Liu S, Perrotti D, Marcucci G and Lee RJ: Efficient delivery of a Bcl-2-specific antisense oligodeoxyribonucleotide (G3139) *via* transferrin receptor-targeted liposomes. J Control Release *112(2)*: 199-207, 2006.

16 Hossen MN, Kajimoto K, Akita H, Hyodo M, Ishitsuka T and Harashima H: Ligand-based targeted delivery of a peptide modified nanocarrier to endothelial cells in adipose tissue. J Control Release *147(2)*: 261-268, 2010.

17 Li Z, Kang HL, Li QM, Che N, Liu ZJ, Li PP, Zhang CC, Liu RG and Huang Y: Ultrathin core-sheath fibers for liposome stabilization. Colloid Surface B *122(122)*: 630-637, 2014.

18 Zhao C, She T, Wang L, Su Y, Qu L, Gao Y, Xu S, Cai S and Shou C: Daucosterol inhibits cancer cell proliferation by inducing autophagy through reactive oxygen species-dependent manner. Life Sci *137*: 37, 2015.

19 Szilágyi G, Simon L, Koska P, Telek G and Nagy Z: Visualization of mitochondrial membrane potential and reactive oxygen species *via* double staining. Neurosci Lett *399(3)*: 206, 2006.

20 Yue Z, Zhou C, Kwak KJ, Wang X, Yung B, Lee LJ, Wang Y, Peng GW and Lee RJ: Efficient siRNA delivery using a polyamidoamine dendrimer with a modified pentaerythritol core. Pharm Res-Dordr *29(6)*: 1627-1636, 2012.

21 Zhou Y, Guo Z, Meng Q, Lu J, Wang N, Liu H, Liang Q, Quan Y, Wang D and Xie J: Cordycepin affects multiple apoptotic pathways to mediate hepatocellular carcinoma cell death. Anticancer Agent Med Chem *17(1)*: 143-149, 2017.

22 Zhang L, Wang K, Lei Y, Li Q, Nice EC and Huang C: Redox signaling: Potential arbitrator of autophagy and apoptosis in therapeutic response. Free Radical Biol Med *89*: 452, 2015.

23 Wang S-J, Gao C and Chen B-A: Advancement of the study on iron metabolism and regulation in tumor cells. Chin J Cancer, *29(4)*: 451-455, 2010.

24 Daniels TR, Delgado T, Helguera G and Penichet ML: The transferrin receptor part II: Targeted delivery of therapeutic agents into cancer cells. Clin Immunol *121(2)*: 159-176, 2006.

Received June 25, 2017
Revised July 10, 2017
Accepted July 26, 2017